

Entanglement entropy dynamics of disordered quantum spin chains

Ferenc Igloi,^{1,2,*} Zsolt Szatmári,^{2,†} and Yu-Cheng Lin^{3,‡}

¹*Wigner Research Centre, Institute for Solid State Physics and Optics, H-1525 Budapest, P.O.Box 49, Hungary*

²*Institute of Theoretical Physics, Szeged University, H-6720 Szeged, Hungary*

³*Graduate Institute of Applied Physics, National Chengchi University, Taipei, Taiwan*

(Dated: March 13, 2012)

By means of free fermionic techniques we study the time evolution of the entanglement entropy, $S(t)$, of a block of spins in the random transverse-field Ising chain after a sudden change of the parameters of the Hamiltonian. We consider global quenches, when the parameters are modified uniformly in space, as well as local quenches, when two disconnected blocks are suddenly joined together. For a non-critical final state, the dynamical entanglement entropy is found to approach a finite limiting value for both types of quenches. If the quench is performed to the critical state, the entropy grows for an infinite block as $S(t) \sim \ln \ln t$. This type of ultraslow increase is explained through the strong disorder renormalization group method.

I. INTRODUCTION

Recently, we have witnessed increasing interest in studying the entanglement properties of quantum many body systems^{1–3} in different disciplines: quantum information, condensed matter physics and quantum field theory. Among the various measures for quantifying entanglement, the von Neumann entropy and its generalizations to Rényi entropies, as well as the entanglement spectrum⁴ have been widely used to obtain useful information about the topological and universal properties of an extended quantum system, in particular at a quantum critical point. For homogeneous, i.e. non-random, systems, many basic results are known in one dimension from conformal field theory,^{5,6} which have been confirmed by exact and numerical calculations on specific models.^{7–11} For a quantum spin chain one generally considers the entanglement entropy, S_ℓ , between a block of ℓ contiguous spins and its complement. For periodic chains, where the block has two boundary points connected with the remainder of the system, the entanglement entropy at the critical point for $\ell \gg 1$ scales as $S_\ell = \frac{c}{3} \ln \ell$, where c is the central charge of the conformal field theory. Away from the critical point, the entropy saturates to a value $S_\ell = \frac{c}{3} \ln \xi$, where $\xi \ll \ell$ (and $\xi \gg 1$) is the correlation length of the system. Recently universal finite-size corrections to the Rényi entropy^{12–15} as well as the entropy of non single-connected blocks have also been studied.^{16,17}

If the couplings in the chain are inhomogeneous, such as there is an internal defect^{8,18–23} or the interactions are quasi-periodic or aperiodic,²⁴ then the prefactor of the critical entanglement entropy, the so called effective central charge, c_{eff} , is generally different from that in the homogeneous system. For chains with random couplings, c_{eff} has been calculated analytically^{25–28} by the strong disorder renormalization group (SDRG) method,²⁹ and numerically by free-fermionic techniques^{30,31} and by the density-matrix renormalization group (DMRG) method.³² Also the entanglement spectrum of random XX chains has been

studied, both by the SDRG method and numerically.³³ We note that the entanglement entropy can be studied even in higher dimensional random quantum systems by numerical implementation of the SDRG method,^{34–36} provided the critical properties of the systems are controlled by infinite-disorder fixed points,^{29,37} as in one dimension.

The nonequilibrium quench dynamics of quantum systems has become a very active field of research, both experimentally and theoretically.³⁸ Dynamical aspects of the entanglement entropy are of interest for their close relationship to the speed of information propagation through an interacting quantum system. In these investigations one changes (some) parameters of the Hamiltonian suddenly, and asks how the entanglement evolves in time.³⁹ One generally distinguishes two types of quenches: global and local quenches. For a global quench the parameters are changed everywhere in space. In this case the entanglement entropy has a linear increase in time t , irrespective of the initial and the final state of the system. This type of dynamics has been explained in terms of quasiparticles (elementary excitations).³⁹ In the other type of quench, known as a local quench, the parameters of the Hamiltonian are changed only locally; for example, a block, which is disconnected from the rest of the system for $t < 0$, is instantaneously connected at time $t = 0$. For the local quench the entanglement entropy at the critical point is found to display a universal logarithmic increase,⁴⁰ $S_\ell = \frac{2c}{3} \ln t$, $t \ll \ell$; this relation has been later derived through conformal invariance.^{41,42}

Concerning dynamical entropy in inhomogeneous systems there have been only a few studies in specific situations.^{20,32,43–45} For local quench the effect of defects has been studied. The defects can be, for example, in the form of couplings between a block, where the entanglement entropy is studied, and the rest of system; for this case, the prefactor of the logarithmic t -dependence of the entanglement entropy is found to be the same as measured in the static case.²⁰ On the other hand, quenched disorder changes the entanglement dynamics in a more drastic way. Previously, the entanglement en-

tropy dynamics of the disordered Heisenberg chain following a global quench was numerically studied,³² where a slow increase of the entropy with time was observed; the numerical data in the time regime ($t \lesssim 500$) obtained by time dependent DMRG suggested that the entropy grows logarithmically with time. The slow propagation of signals in disordered system has been later supported by theoretical work,⁴³ in which, by means of the generalized Lieb-Robinson bound,⁴⁴ a bound for time evolution of the entanglement entropy is derived in the form: $S_\ell(t) \leq c_1 + c_2 \log(\ell|t|)$, with c_1 and c_2 being constants.

In this paper we revisit the problem of the entanglement entropy dynamics in disordered quantum spin chains. The model we consider is the random transverse-field Ising chain. Our study extends previous investigations on entanglement dynamics in disordered systems in several respects: (i) we study the entanglement dynamics both at the critical point and in the off-critical phases, using numerically exact free-fermionic techniques; (ii) we consider both global and local quenches; (iii) we study the time evolution for a very long period of time and obtain the long-time asymptotics for finite systems; (iv) furthermore, we explain the numerical findings based on SDRG.

The structure of the rest of the paper is as follows. In section II we introduce the model, describe its basic equilibrium properties and outline the method of calculation. Results of the entanglement entropy dynamics after global and local quenches are presented in sections III and IV, respectively. The results are discussed in section V.

II. THE MODEL

The model we consider is the quantum Ising chain of length L defined by the Hamiltonian:

$$\mathcal{H} = - \sum_{i=1}^L J_i \sigma_i^x \sigma_{i+1}^x - \sum_{i=1}^L h_i \sigma_i^z, \quad (1)$$

in terms of the Pauli matrices $\sigma_i^{x,z}$ at site i . In this paper we will take periodic boundary conditions so that $\sigma_{L+1} = \sigma_1$. The homogeneous model with the couplings $J_i = 1$ and the transverse fields $h_i = \tilde{h}$ is in the disordered (ordered) phase for $\tilde{h} > 1$ ($\tilde{h} < 1$), and the quantum critical point is located at $\tilde{h} = 1$.⁴⁶ The critical point of the model is described by a conformal field theory with a central charge $c = 1/2$. In the random model with quenched disorder, the J_i and the h_i are position dependent, and are independent random numbers taken from uniform distributions in the intervals $[0, 1]$ and $[0, 1]h$, respectively. The random model is in the disordered (ordered) phase for $h > 1$ ($h < 1$) and the random quantum critical point is at $h = 1$. The equilibrium critical properties of the random chain has been studied by the SDRG method,⁴⁷ and the random quantum critical point is found to be controlled by an infinite-disorder

fixed point, at which the scaling is extremely anisotropic, so that the typical length, ξ , and the typical time, τ , is related as

$$\ln \tau \sim \xi^\psi, \quad (2)$$

with an exponent $\psi = 1/2$.

In this work we study the entanglement entropy of a block of contiguous spins sitting on sites $1, 2, \dots, \ell$ in the chain; the entanglement entropy is defined as $S_\ell = -\text{Tr}_\ell[\rho_\ell \ln \rho_\ell]$ in terms of the reduced density matrix: $\rho_\ell = \text{Tr}_{i>\ell} |0\rangle\langle 0|$, where $|0\rangle$ denotes the ground state of the complete system with L sites. In the calculation we make use of the fact that the Hamiltonian in Eq.(1) can be expressed in terms of free fermions,^{46,48} and the density matrix of the corresponding free fermionic system is then obtained from its correlation matrix.^{7,8,11} This calculation for a system in equilibrium is straightforward. In the nonequilibrium case with quench dynamics one has two Hamiltonians, say \mathcal{H}_0 for $t < 0$ and \mathcal{H} for $t > 0$, both in the form of Eq.(1) but with different parameters. The time-evolution of the density matrix is governed by \mathcal{H} , as $\rho(t) = \exp(-i\mathcal{H}t)\rho\exp(i\mathcal{H}t)$, but its matrix elements are calculated through the eigenstates of the initial Hamiltonian \mathcal{H}_0 . Details of the calculation of the dynamical entropy can be found in Ref. 20.

In the following, we first present results for global quenches and then for local quenches. In each case, we will first briefly discuss the homogeneous model to compare with our main results for the random chain, which will be given subsequently.

III. GLOBAL QUENCH

In a global quench the parameters of the Hamiltonian are modified everywhere in space. Concerning the Hamiltonian in Eq. (1), we modify the transverse fields, but leave the couplings unaltered in the quench procedure.

A. Homogeneous chain

In the homogeneous chain the transverse fields are changed from \tilde{h}_0 to \tilde{h} and we measure $S_\ell(t)$ in a chain of total length $L = 256$ for various sizes of the block ℓ . Different combinations of \tilde{h}_0 and \tilde{h} are considered, including quenches from an ordered state to another ordered state [Fig. 1 (a)], from a disordered state to another disordered state [Fig. 1 (d)] and quenches through the critical point [Fig. 1 (b) and 1 (c)].

In each combination of \tilde{h}_0 and \tilde{h} the dynamical entropy has a similar behavior. After a linearly increasing period, $\mathcal{S} = \alpha(\tilde{h}_0, \tilde{h})t$, the entropy saturates to a value $\mathcal{S} = \beta(\tilde{h}_0, \tilde{h})\ell$, and decreases subsequently. This time dependence of $\mathcal{S}(t)$ repeats quasi-periodically, which is different from the case in the thermodynamic limit $L \rightarrow \infty$, where the entropy remains constant after it saturates.^{39,49}

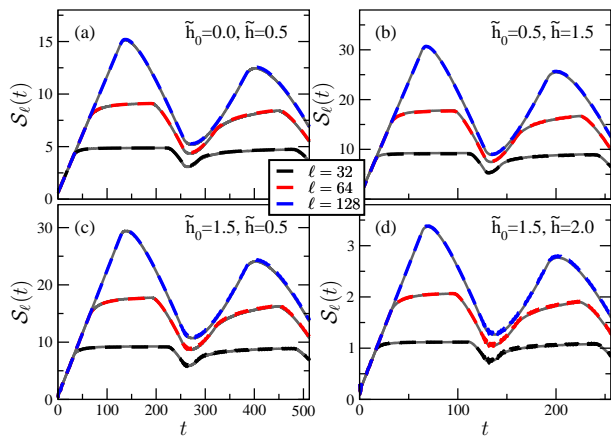


FIG. 1: (Color online) Entanglement entropy of a block of ℓ contiguous spins in the homogeneous chain of length $L = 256$ after a quench from a state with \tilde{h}_0 to a state with \tilde{h} . Results of the semiclassical calculation are given by the gray curves.

We recall that the exact values of $\alpha(\tilde{h}_0, \tilde{h})$ and $\beta(\tilde{h}_0, \tilde{h})$ for $L \rightarrow \infty$ and for a large ℓ have been calculated;⁴⁹ for the special case, when the quench is performed to the critical state with $\tilde{h} = 1$, the coefficient $\alpha(\tilde{h}_0, \tilde{h} = 1)$ can be calculated in a closed form.⁵⁰ Following a semiclassical approach in terms of ballistically moving quasiparticles formulated in Ref. 51, we are able to calculate the dynamical entropy for the finite chain. The quasiparticles are Fourier transforms of kink states, created as a pair of entangled free fermions with quasimomenta $\pm p$.^{39,51} With energy ϵ_p , a ballistically moving quasiparticle has the semiclassical velocity $v_p = \frac{\partial \epsilon_p}{\partial p}$. These quasiparticles are created homogeneously in space at $t = 0$ with an occupation probability f_p . If a pair of entangled particles arrive simultaneously in the block and outside the block, they will contribute $s_p = -(1 - f_p) \ln(1 - f_p) - f_p \ln f_p$ to the entanglement entropy. Summing up the contributions from all quasiparticles (i.e. over positions and quasimomenta) we obtain the dynamical entropy as shown in Fig. 1 by the grey curves. As can be seen, the results obtained from this semiclassical approach fit our numerically exact data perfectly, even for a large range of t .

B. Random chains

Now we turn to the disordered chain with random couplings and random fields. In our quench procedure, the set of couplings $\{J_i\}$ for a given sample remains unaltered, whereas the width of the transverse-field distribution is changed from h_0 ($t < 0$) to h ($t \geq 0$). We consider quenches in the off-critical phases as well as quenches to the critical point. In most of our calculations the widths h_0 and h are different; we keep the local transverse field on each site correlated before and after the quench, but change the relative magnitude by

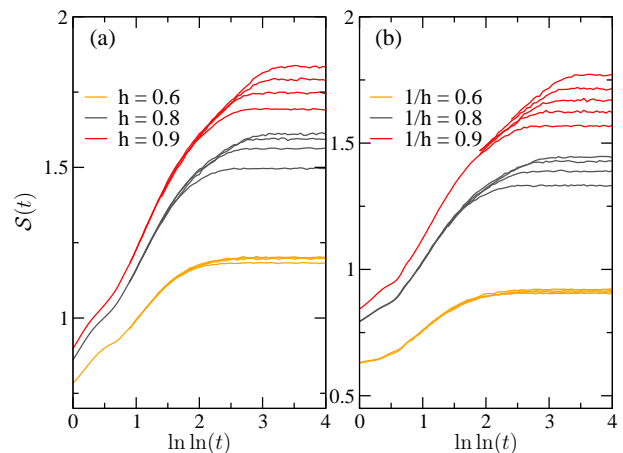


FIG. 2: (Color online) Disorder-averaged entanglement entropy for several global quenches performed outside the critical point of random chains, plotted against double logarithmic time $\ln \ln t$. (a): quench from a fully ordered initial state with $h_0 \rightarrow 0$ to an ordered state with $h = 0.6, 0.8$ and 0.9 ; (b): quench from a fully disordered initial state with $1/h_0 \rightarrow 0$ to a disordered state with $1/h = 0.6, 0.8$ and 0.9 . System sizes ranging from $L = 32$ to $L = 192$ are considered; the bigger the system, the higher the value of the entropy at large t .

$h_i(t < 0)/h_i(t \geq 0) = h_0/h, \forall i$. We also consider the case where the quench is performed at the critical point, i.e. $h_0 = h = 1$; for this case we use two independent sets of random variables for the transverse fields before and after the quench.

We have calculated the disorder-averaged entanglement entropy between two blocks of length $\ell = L/2$ in a chain for different system sizes up to $L = 256$. We have used at least 10,000 disordered realizations to obtain the disorder average.

The time-dependence of the average entanglement entropy for quenches to a non-critical state and for quenches to the critical point is qualitatively different. Below we present results for these two cases separately.

1. Quench to non-critical states

We performed quenches from a fully ordered initial state $h_0 \rightarrow 0$ to ordered states with $0 < h < 1$ and quenches from a fully disordered initial state $h_0 \rightarrow \infty$ to disordered states with finite $h > 1$. Results for the disorder-averaged entanglement entropy as a function of time for quenches in the ordered phase with parameters $h = 0.6, h = 0.8$ and $h = 0.9$ are shown in Fig. 2(a). Results for quenches in the disordered phase with parameters $1/h = 0.6, 1/h = 0.8$ and $1/h = 0.9$ are shown in Fig. 2(b). In both cases the time variation is extremely slow, therefore we have used double-logarithmic time scales in the figures.

As seen in the figures, the entanglement entropy for

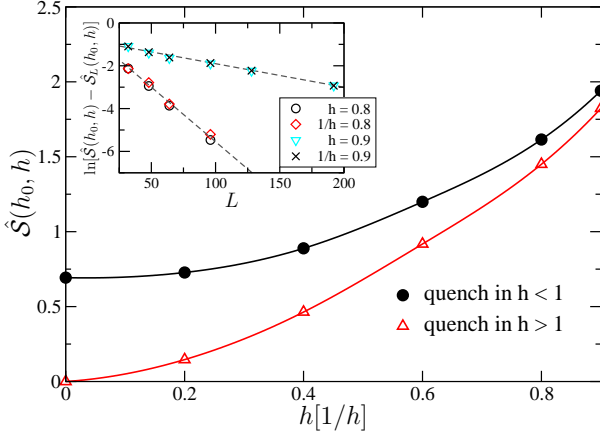


FIG. 3: (Color online) Saturation values of the entanglement entropy at $t \rightarrow \infty$ and for large L , for quenches from a fully ordered initial state $h_0 \rightarrow 0$ to an ordered final state, as well as from a fully disordered state $h_0 \rightarrow \infty$ to another disordered state $h > 1$. The results for quenches in the region $h < 1$ are plotted against h , while the results for quenches in $h > 1$ are plotted against $1/h$. Inset: Finite-size corrections to the saturation value of the entropy for a quench from $h_0 \rightarrow 0$ to $h = 0.8$ and $h = 0.9$, as well as from $1/h_0 \rightarrow 0$ to $1/h = 0.8$ and $1/h = 0.9$. The asymptotic values in the large- L limit used for this plot are $\hat{S}(0, 0.8) = 1.615$, $\hat{S}(0, 0.9) = 1.941$, $\hat{S}(\infty, 0.8^{-1}) = 1.450$ and $\hat{S}(\infty, 0.9^{-1}) = 1.823$.

different system sizes L saturates to a value $\hat{S}_L(h_0, h)$ at large t . Furthermore, this saturation value converges to a L -independent value for large L , i.e. $\lim_{L \rightarrow \infty} \hat{S}_L(h_0, h) = \hat{S}(h_0, h)$. This asymptotic value for $L \rightarrow \infty$ and $t \rightarrow \infty$ is larger if the final state is closer to critical point $h = 1$, as shown in Fig. 3. Furthermore, we have obtained an exponential relation for the finite-size correction term, given by $\hat{S}(h_0, h) - \hat{S}_L(h_0, h) \approx \exp(-L/\xi(h))$, as illustrated in the inset of Fig. 3 for quenches from $h_0 \rightarrow 0$ to $h = 0.8$ and $h = 0.9$, as well as for “dual process”, starting with $1/h_0 \rightarrow 0$ and ending at $1/h = 0.8$ and $1/h = 0.9$. From this relation we have estimated the values of $\xi(h)$ for h close to the critical point, and obtain $\xi(0.8) \approx \xi(1.25) = 19.8(8)$, and $\xi(0.9) \approx \xi(1.11) = 95.5(5)$, which are in agreement with the scaling form of the equilibrium correlation length of the random transverse-field Ising chain:⁴⁷ $\xi(h) \sim |h - 1|^{-2}$. For this study we have used several initial states in the ordered and disordered phases, and the same scaling form for $\xi(h)$ has been found.

2. Quench to the critical point

Results for the time dependence of the average entanglement entropy after global quenches from a fully ordered state ($h_0 \rightarrow 0$) and a fully disordered state ($1/h_0 \rightarrow 0$) to the critical state are shown in Fig. 4.

The entanglement entropy for the quench to the critical point increases with time up to $\tau(L)$, after which it sat-

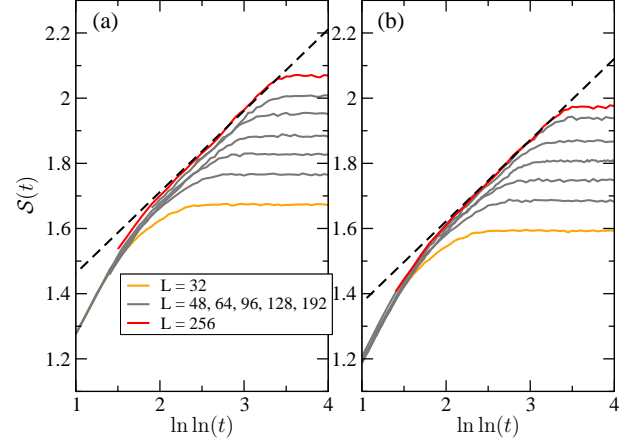


FIG. 4: (Color online) Average dynamical entropy after a quench to the critical point of the random chain. (a): The initial state is fully ordered ($h_0 \rightarrow 0$), (b): the initial state is fully disordered ($1/h_0 \rightarrow 0$). The dashed lines in both (a) and (b) have slope 0.25.

urates to a value. The asymptotic values of the entropy for $t > \tau(L)$ increase monotonously with L . Analyzing the numerical data in Fig. 5 we obtain a logarithmic L -dependence:

$$\hat{S}_L(h_0, 1) = s(h_0) + b \ln L, \quad (3)$$

where the prefactor of the logarithm is found to be independent of the initial state: $b \approx 0.173 \approx \ln 2/4$; This is different than the prefactor for the equilibrium entanglement entropy: $c_{\text{eff}}/3 = \ln 2/6$.²⁵

For $t < \tau(L)$, we have found a double-logarithmic growth of the entropy in time given by

$$S(t) = s + a \ln \ln t, \quad (4)$$

with $a \approx 0.25$, which is also independent of the initial state. This ultraslow growth of the entropy in time reflects the nature of an infinite-disorder fixed point which is characterized by the activated dynamics $\ln \tau \sim L^{\psi_{\text{ne}}}$. Combining Eq. (3) and Eq. (4), we obtain the exponent $\psi_{\text{ne}} = b/a = 0.69(3)$, which is larger than the exact value, $\psi = 1/2$, known for the equilibrium case.

We have repeated the calculation for the case when the initial state is also critical with $h_0 = 1$. A double-logarithmic growth of $S(t)$ in time and the same exponent ψ_{ne} were obtained.

IV. LOCAL QUENCH

In the local quench process, we consider the entanglement entropy of a block corresponding to one half of the chain with $\ell = L/2$, which is disconnected from the rest of the chain, with $J_L = J_{L/2} = 0$, for $t < 0$, and is joined up at $t = 0$ with $J_L = J_{L/2} \neq 0$; the transverse field

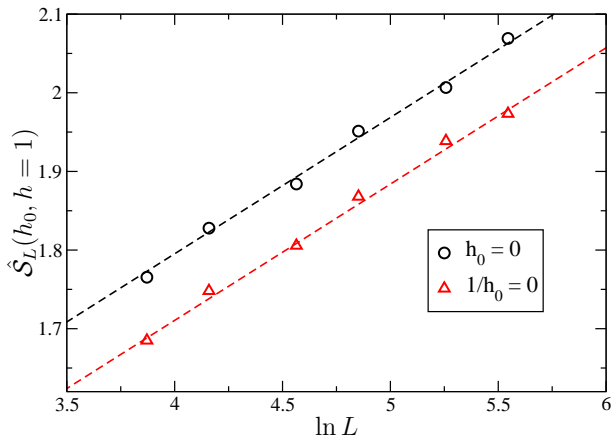


FIG. 5: (Color online) Saturation value of the average dynamical entropy as a function of $\ln L$, for quenches from a fully ordered state $h_0 \rightarrow 0$ and a fully disordered state $h_0 \rightarrow \infty$ to the critical point. The straight dashed lines have the same slope $\ln 2/4$.

remains unchanged after the quench. We study the time evolution of the entanglement entropy for $t > 0$.

A. Homogeneous chain

For the homogeneous chain of length L the couplings joining the block to the rest of the system for $t > 0$ are $J_L = J_{L/2} = 1$. We have calculated the entropy dynamics after a local quench for different values of the transverse field, including the critical value and the values for ordered as well as disordered phases; the results for $L = 256$ are presented in Fig. 6.

At the critical point, $\tilde{h} = 1$, the entanglement entropy oscillates with a period $t = L/2$, and this periodic function can be well described as

$$S(t) = 2\frac{c}{3} \ln \left| \frac{L}{2\pi} \sin \frac{2\pi t}{L} \right| + \text{cst.}, \quad (5)$$

which was first found in Ref. 20, and has been derived recently through conformal invariance.⁴²

If the quench is performed outside the critical point the dynamical entropy grows only up to a finite limiting value, as shown in Fig. 6, both in the ordered phase (upper panel) and in the disordered phase (lower panel). The amplitudes of oscillations of $S(t)$ are reduced for large- L and for large t , and the limiting saturation value is of the order of $2\frac{c}{3} \ln \xi_{\text{hom}}$, with the correlation length, $\xi_{\text{hom}} \simeq |1 - \tilde{h}|^{-1}$, close to the critical point.

B. Random chains

For a random chain, the couplings are independent random variables taken from the uniform distribution in the

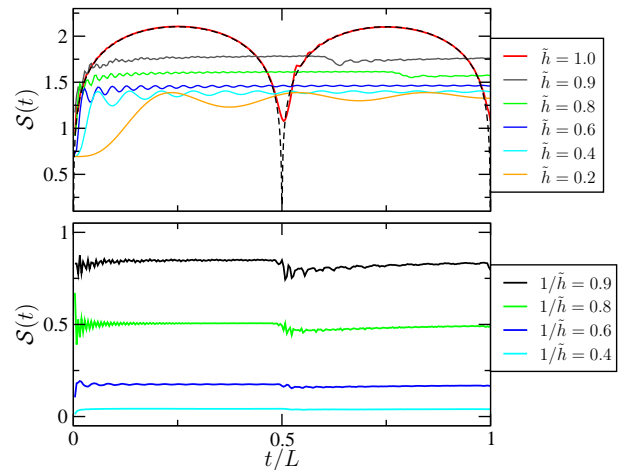


FIG. 6: (Color online) Dynamical entanglement entropy of the homogeneous system after a local quench versus the rescaled time t/L , for $L = 256$. Upper panel: quench to a ordered phase and to the critical point. For the latter case the conformal result in Eq. (5) is shown by the dashed line. Lower panel: quench to the disordered phase.

interval $[0, 1]$. The two couplings J_L and $J_{L/2}$ are removed for $t < 0$, and are instantaneously joined to the chain at $t = 0$. For the transverse fields we use the distribution described in Sec. II.

1. Quench outside the critical point

We first discuss the time evolution of the disorder-averaged entropy in the non-critical phases. The results for two examples in the ordered phase are presented in Fig. 7 (a) and 7 (b), and for quenches in the disordered phase are in Fig. 7 (c) and 7 (d). Due to extremely slow time evolution, the data for different system sizes L are plotted against $\ln \ln t$.

In the long-time regime, the entropy approaches an L -dependent saturation value $\hat{S}_L(h)$, which converges for large sizes: $\lim_{L \rightarrow \infty} \hat{S}_L(h) = \hat{S}(h)$. As shown in Fig. 7(e), the value $\hat{S}(h)$ increases monotonously as the critical point is approached; furthermore, this asymptotic value at each h is smaller than the asymptotic value of the entropy after a global quench to an off-critical phase.

2. Quench at the critical point

The dynamical entropy after a local quench at the critical point is shown in Fig. 8 for different lengths of the chain. The overall characteristics of the entropy in this figure is similar to that in Fig. 4 obtained after a global quench.

For a fixed length L , there is a characteristic time $\tau(L)$, after which the average entropy is saturated to $\hat{S}_L(1)$. These saturation values follow a logarithmic L -

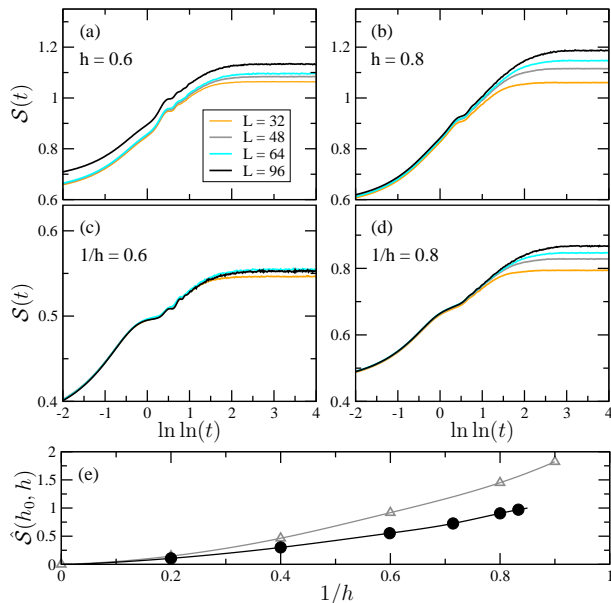


FIG. 7: (Color online) (a)-(d): Entanglement entropy versus double logarithmic time after local quenches performed in off-critical phases of the random chain for different lengths. (e): The data points with filled black circles are the asymptotic results for large L and large t in the disordered phase. The data in gray are results for global quenches in the disordered phase (also shown in Fig. 3), given for comparison.

dependence: $\hat{S}_L(1) = s_1 + b_1 \ln L$, for large sizes [see the inset in Fig. 8]. Here the prefactor of the logarithm is estimated as $b_1 \approx 0.139 \approx \ln 2/5$, which is smaller than the prefactor for a global quench to the criticality: $b \approx \ln 2/4$, and is slightly larger than the prefactor of the equilibrium entropy: $c_{\text{eff}}/3 = \ln 2/6$.

For $t < \tau(L)$, the average entropy has a double-logarithmic time-dependence: $\mathcal{S}(t) = s_1 + a_1 \ln \ln t$ with a prefactor $a \approx 0.16(2)$. Based on the argument for the global quench in sec. III B 2, we obtain $\ln \tau(L) \sim L^{\psi_{\text{ne}}^{\text{loc}}}$ with the exponent $\psi_{\text{ne}}^{\text{loc}} = 0.87(3)$; this exponent is larger than the exponent $\psi_{\text{ne}} = 0.69(3)$, obtained for a global quench.

V. DISCUSSION

We have studied the time-evolution of the entanglement entropy in the random transverse-field Ising chain after a global and a local quench. The obtained results are strikingly different from that calculated for the homogeneous version of the system. The slow dynamics of entanglement in a disordered quantum chain was observed in a previous numerical study,³² and has been supported by theoretical work.⁴³ Our present numerical study provides clear evidence showing that this dynamics at the critical point is ultraslow and in a double-logarithmic form.

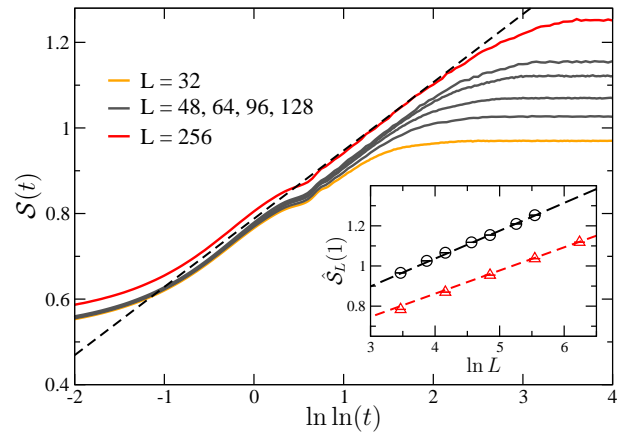


FIG. 8: (Color online) Disorder-averaged dynamical entropy after a local quench at the critical point of the random chain. Inset: The asymptotic values at $t \rightarrow \infty$ (black circles) for different system sizes, compared with the static entanglement entropy between two halves of the chain (red triangles). The black dashed line has slope $\ln 2/5$, and the red dashed line for the static case has slope $\ln 2/6$.

To explain the difference observed in the time evolution of the entanglement entropy in homogeneous and in random chains, we apply the semiclassical quasiparticle picture³⁹ to both cases. In the homogeneous case⁵¹, the quasiparticles are related to kinks in the form of domain walls between differently aligned spin configurations, which are created as entangled fermion pairs with quasimomenta $\pm p$ moving ballistically in the opposite directions. These entangled quasiparticles will contribute to the entanglement entropy between two regions if one particle arrives in one of the regions and the other reaches simultaneously the other region. From the occupation probability of the modes with p , one can calculate the entanglement entropy, as discussed in sec. III A, and can understand the characteristics of the time evolution of the entanglement entropy.

The properties of the quasiparticles and the dynamics of the entanglement entropy in the random transverse-field Ising chain can be understood from the asymptotically exact SDRG. As known from the SDRG, the scaling properties of the random chain are described by an infinite-disorder fixed point, at which disorder fluctuations are completely dominant while quantum fluctuations are negligible.^{29,47} The ground state of the random chain consists of a set of non-overlapping effective spin clusters, each of which has a characteristic energy scale Δ_{cl} , given by the excitation energy of the cluster. The size of a cluster, ℓ_{cl} , is finite in a non-critical phase, its typical value defines the correlation length ξ . (In the ordered phase, there is a giant cluster which is embedded in finite clusters). At the critical point, where ξ is divergent, for the largest clusters we have asymptotically: $|\ln \Delta_{\text{cl}}| \sim \ell_{\text{cl}}^{1/2}$ [cf. Eq. (2)]. The energy-length scaling described above is also related to Sinai-diffusion

in stochastic processes,^{52–54} which explains ultraslow dynamics in one-dimensional disordered environments.

The spins in a cluster defined in SDRG are maximally entangled. Each cluster contributes to the entanglement entropy between a block and the rest of the system by an amount of $s_{\text{cl}} = \ln 2$ as long as it crosses the boundary of the block. In equilibrium, the disorder-averaged entanglement entropy at the critical point, where the correlation length is divergent, is obtained by summing up contributions of all clusters in the ground state, $\mathcal{S}_\ell = \sum_{\ell_{\text{cl}} < \ell} s_{\text{cl}}$, yielding $\mathcal{S}_\ell = \frac{\ln 2}{6} \ln \ell$ for a block of length ℓ .²⁵

In the nonequilibrium case, the cluster formations in the SDRG picture are time-dependent. The time span that quantum correlations between different spins to be built up is the time for the formation of the cluster containing these spins, and is given by $t_{\text{cl}} \sim \Delta_{\text{cl}}^{-1}$. The time span t_{cl} also corresponds to the time in which a signal emitted at one end of the cluster arrives at the other end of the cluster via a Sinai diffusion. The time-dependent entanglement entropy $\mathcal{S}_\ell(t)$ at the critical point can be obtained by summing over contribution of all entangled clusters up to time t : $\mathcal{S}_\ell(t) = \sum_{t_{\text{cl}} < t} s_{\text{cl}} \sim \ln \xi(t) \sim \ln \ln t$, where $\xi(t)$ is a nonequilibrium length-scale, given by $\xi(t) \sim \ln(t)^{1/\psi_{\text{ne}}}$. In the long-time limit when the cluster of size $\ell_{\text{cl}} \lesssim \ell$ are already formed, the entanglement entropy saturates to a value that is proportional to $\ln \ell$. The explanation through the SDRG description holds both for global and local quenches. The main difference between global and local quenches is the excess energy is finite in a local quench, while it is extensive in a global quench. When the excess energy is extensive, high energy excitations also contribute to the dynamics of entanglement entropy and may be responsible for the nonuniversal short-time behavior; this is similar to the situation in nonrandom gapless systems after a

global quench: conformal field theory describes the linear growth of the entropy, although excited states strongly influence the nonequilibrium dynamics.³⁹

The ultraslow behavior of the dynamical entanglement entropy observed in the random transverse-field Ising chain should be generic for random quantum systems whose critical point is governed by an infinite-disorder fixed point; this includes the random XY -chain (which has, in fact, an exact mapping with the Ising chain),¹¹ the random XXZ -chain,⁵⁵ and the random quantum Potts chain.⁵⁶ Besides, the quantum criticality of the random transverse-field Ising model even in higher dimensions is also controlled by an infinite-disorder fixed point.^{57–62} It has been found that at this critical point in higher dimensions there is a singular contribution to the entanglement entropy of the form $\Delta \mathcal{S}_\ell \sim \log \ell$ for a block in a hypercube form of linear size ℓ ;³⁶ this singularity is shown to be related to the presence of corners. In the dynamical process this corner contribution is expected to increase in a double-logarithmic fashion.

Note added: After submitting this paper we noticed the preprint by Levine *et al*⁶³, in which the time-dependence of the full counting statistics in a disordered fermion system is studied, which is closely related to the local quench problem discussed in this work.

Acknowledgments

We are grateful to I. Peschel and to H. Rieger for discussions. FI acknowledges support from the Hungarian National Research Fund under grant No OTKA K75324 and K77629; he also acknowledges travel support from the NCTS in Taipei, and visitors programs at National Chengchi University and Academia Sinica. YCL was supported by the NSC (Taiwan) under Grant No. 98-2112-M-004-002-MY3.

* Electronic address: igloi.ferenc@wigner.mta.hu

† Electronic address: zsolt.szatmari@me.com

‡ Corresponding author: yc.lin@nccu.edu.tw

¹ L. Amico, R. Fazio, A. Osterloh, and V. Vedral, *Rev. Mod. Phys.* **80**, 517 (2008).

² P. Calabrese, J. Cardy and B. Doyon (Eds.), *Entanglement entropy in extended quantum systems* (special issue), *J. Phys. A* **42** 500301 (2009).

³ J. Eisert, M. Cramer, and M. B. Plenio, *Rev. Mod. Phys.* **82**, 277 (2010).

⁴ P. Calabrese and A. Lefevre, *Phys. Rev. A* **78**, 32329 (2008).

⁵ C. Holzhey, F. Larsen, and F. Wilczek, *Nucl. Phys. B* **424**, 443 (1994).

⁶ P. Calabrese and J. Cardy, *J. Stat. Mech.* (2004) P06002.

⁷ G. Vidal, J. I. Latorre, E. Rico, and A. Kitaev, *Phys. Rev. Lett.* **90**, 227902 (2003); J. I. Latorre, E. Rico, and G. Vidal, *Quantum Inf. Comput.* **4**, 048 (2004).

⁸ I. Peschel, *J. Phys. A: Math. Gen.* **36**, L205 (2003).

⁹ B.-Q. Jin and V.E. Korepin, *J. Stat. Phys.* **116**, 79 (2004);

A. R. Its, B.-Q. Jin and V.E. Korepin, *Fields Institute Communications, Universality and Renormalization* [editors I. Bender and D. Kreimer] **50**, 151 (2007).

¹⁰ I. Peschel, *J. Stat. Mech.* P12005 (2004).

¹¹ F. Iglói and R. Juhász, *Europhys. Lett.* **81**, 57003 (2008).

¹² N. Laflorencie, E. S. Sørensen, M. S. Chang, and I. Affleck, *Phys. Rev. Lett.* **96**, 100603 (2006).

¹³ P. Calabrese, M. Campostrini, F. Essler, B. Nienhuis, *Phys. Rev. Lett.* **104**, 095701 (2010); P. Calabrese and F. H. L. Essler, *J. Stat. Mech.* P08029 (2010).

¹⁴ J. Cardy and P. Calabrese, *J. Stat. Mech.*, P04023 (2010).

¹⁵ F. C. Alcaraz, M. I. Berganza, G. Sierra, *Phys. Rev. Lett.* **106**, 201601 (2011); M. I. Berganza, F. C. Alcaraz, G. Sierra, *J. Stat. Mech.*, P01016 (2012).

¹⁶ V. Alba, L. Tagliacozzo, P. Calabrese, *Phys. Rev. B* **81**, 060411(R) (2010).

¹⁷ F. Iglói and I. Peschel, *EPL* **89**, 40001 (2010).

¹⁸ I. Peschel and J. Zhao, *J. Stat. Mech.* P11002 (2005).

¹⁹ G. C. Levine and D. J. Miller, *Phys. Rev. B* **77** 205119 (2008).

- ²⁰ F. Iglói, Zs. Szatmári, and Y.-C. Lin, Phys. Rev. B **80**, 024405 (2009).
- ²¹ V. Eisler, I. Peschel, Annalen der Physik, 522, 679 (2010).
- ²² P. Calabrese, M. Mintchev, and E. Vicari, J. Phys. A: Math. Theor. 45 105206 (2012).
- ²³ I. Peschel, V. Eisler, arXiv:1201.4104.
- ²⁴ F. Iglói, R. Juhász, and Z. Zimborás, Europhys. Lett. **79**, 37001 (2007).
- ²⁵ G. Refael and J. E. Moore, Phys. Rev. Lett. **93**, 260602 (2004).
- ²⁶ R. Santachiara, J. Stat. Mech. Theor. Exp. L06002 (2006).
- ²⁷ N. E. Bonesteel and K. Yang, Phys. Rev. Lett. **99**, 140405 (2007).
- ²⁸ G. Refael and J. E. Moore, Phys. Rev. B **76**, 024419 (2007).
- ²⁹ For a review, see: F. Iglói and C. Monthus, Physics Reports **412**, 277, (2005).
- ³⁰ N. Laflorencie, Phys. Rev. B **72** 140408 (R) (2005).
- ³¹ F. Iglói and Y.-C. Lin, J. Stat. Mech. P06004 (2008).
- ³² G. De Chiara, S. Montangero, P. Calabrese, R. Fazio, J. Stat. Mech., L03001 (2006).
- ³³ M. Fagotti, P. Calabrese, and J. E. Moore, Phys. Rev. B **83**, 045110 (2011).
- ³⁴ Y.-C. Lin, F. Iglói and H. Rieger, Phys. Rev. Lett. **99**, 147202 (2007).
- ³⁵ R. Yu, H. Saleur and S. Haas, Phys. Rev. B **77**, 140402 (2008).
- ³⁶ I. A. Kovács and F. Iglói, arXiv:1108.3942.
- ³⁷ D.S. Fisher, Physica A **263**, 222 (1999).
- ³⁸ For a review, see: J. Dziarmaga, Advances in Physics **59**, 1063 (2010).
- ³⁹ P. Calabrese and J. L. Cardy, J. Stat. Mech. P04010 (2005).
- ⁴⁰ V. Eisler and I. Peschel, J. Stat. Mech. P06005 (2007).
- ⁴¹ P. Calabrese and J. L. Cardy, J. Stat. Mech. P10004 (2007).
- ⁴² J.-M. Stéphan and J. Dubail, J. Stat. Mech. P08019 (2011).
- ⁴³ C. K. Burrell, T. J. Osborne, Phys. Rev. Lett. **99**, 167201 (2007).
- ⁴⁴ E. H. Lieb and D.W. Robinson, Commun. Math. Phys. **28**, 251 (1972).
- ⁴⁵ C. K. Burrell, J. Eisert, T. J. Osborne, Phys. Rev. A **80**, 052319 (2009); J. Allcock and N. Linden, Phys. Rev. Lett. **102**, 110501 (2009); E. Khatami, M. Rigol, A. Relaño, A. M. Garcia-Garcia, arXiv:1103.0787; G. P. Brandino, A. De Luca, R.M. Konik, G. Mussardo, arXiv:1111.6119; J. Hide, J. Phys. A: Math. Theor. 45 115302 (2012).
- ⁴⁶ P. Pfeuty, Phys. Lett. A **72**, 245 (1979).
- ⁴⁷ D.S. Fisher, Phys. Rev. Lett. **69**, 534 (1992); Phys. Rev. B **51**, 6411 (1995).
- ⁴⁸ E. Lieb, T. Schultz and D. Mattis, Annals of Phys. **16**, 407 (1961).
- ⁴⁹ M. Fagotti and P. Calabrese, Phys. Rev. A **78** 010306(R) (2008).
- ⁵⁰ V. Eisler, F. Iglói and I. Peschel, J. Stat. Mech. P02011 (2009).
- ⁵¹ H. Rieger and F. Iglói, Phys. Rev. B **84**, 165117 (2011).
- ⁵² G. Ya. Sinai, Theor. Prob. Appl. **27**, 256 (1982).
- ⁵³ D. Fisher, P. Le Doussal, C. Monthus, Phys. Rev. Lett. **80** 3539 (1998); Phys. Rev. E **59** 4795 (1999).
- ⁵⁴ F. Iglói and H. Rieger, Phys. Rev. E **58**, 4238 (1998).
- ⁵⁵ D.S. Fisher, Phys. Rev. B **50**, 3799 (1995).
- ⁵⁶ T. Senthil and S. N. Majumdar, Phys. Rev. Lett. **76**, 3001 (1996); E. Carlon, P. Lajkó and F. Iglói, Phys. Rev. Lett. **87**, 277201 (2001).
- ⁵⁷ C. Pich, A. P. Young, H. Rieger, and N. Kawashima, Phys. Rev. Lett. **81**, 5916 (1998).
- ⁵⁸ Y.-C. Lin, N. Kawashima, F. Iglói, and H. Rieger, Prog. Theor. Phys. Suppl. **138**, 479 (2000).
- ⁵⁹ I. A. Kovács and F. Iglói, Phys. Rev. B **82**, 054437 (2010).
- ⁶⁰ I. A. Kovács and F. Iglói, Phys. Rev. B **83**, 174207 (2011).
- ⁶¹ I. A. Kovács and F. Iglói, J. Phys.: Condens. Matter **23**, 404204 (2011).
- ⁶² C. Monthus and Th. Garel, J. Phys. A **45**, 095002 (2012); J. Stat. Mech. (2012) P01008.
- ⁶³ G. C. Levine, M. J. Bantegui and J. A. Burg, arXiv:1201.3933.